Research Square

Preprints are preliminary reports that have not undergone peer review.
They should not be considered conclusive, used to inform clinical practice,
or referenced by the media as validated information.

# Raw material procurement in northwest Sierra Morena during the Middle Palaeolithic: quartz exploitation at La Sima Cave (Constantina, Seville, SW Spain)

**Cañete-Gómez Marta**
University of Córdoba
**Caro-Gómez José Antonio**
University of Córdoba
**Borja-Barrera César**
Universidad de Sevilla
**Álvarez-García Genaro**
Sociedad Espeleológica Geos (Exploraciones e Investigaciones Subterráneas)
**Medina-Luque Eusebio**
University of Córdoba
**Díaz del Olmo Fernando**
Universidad de Sevilla
**Recio-Espejo José Manuel**
University of Córdoba
**Gómez-Sánchez María Leticia**
Universidad de Málaga
**Garrido-Anguita Juan Manuel**
jmgarrido@uco.es

University of Córdoba

**Research Article**

**Keywords:** Middle Palaeolithic, Upper Pleistocene, raw materials, quartz, Sierra Morena, La Sima Cave

**Posted Date:** July 3rd, 2026

**DOI:** https://doi.org/10.21203/rs.3.rs-10140225/v1

**License:** This work is licensed under a Creative Commons Attribution 4.0 International License. Read Full License

**Additional Declarations:** No competing interests reported.

## Abstract

***Context*** La Sima Cave (SW Spain) has been systematically excavated from 2011 to 2022. It presents a broad stratigraphy, including Middle Palaeolithic levels (40–50 ka BP) with abundant fauna and lithic industry of diverse lithologies: quartz, quartzite, chert, etc.

***Objectives*** This study aims to characterise and assess the representativeness of these raw materials, identify source areas within the surrounding landscape, and assess the mobility and landscape connectivity factors between them.

**Methods** Lithological characterisation was conducted at both macroscopic and microscopic scales. Geological and geomorphological mapping was evaluated to identify connectivity routes between the site and the procurement sources (quartz outcrops, and Guadalquivir River terraces for quartzites and chert). Finally, the resulting data were then integrated into a GIS framework.

***Results*** Five potential primary quartz procurement sources have been located, and it has been established that the quartzite and chert originate from the Guadalquivir fluvial deposits. Various maps displaying optimal routes, accessibility, and accumulated costs within the potential resource catchment areas have been generated. Furthermore, 24 quartz thin sections were analysed and characterised; multivariate statistical methods were applied to these results, allowing for the proposal of several distinct assemblages.

***Conclusions*** These data suggest that human mobility strategies within this territory would have focused on two potential pathways for procuring lithic resources: a) a primary strategy involving quartz exploitation from nearby outcrops (< 10 km); and b) an alternative axis aimed at acquiring higher-quality raw materials (quartzite and chert) from the fluvial terraces of the Guadalquivir River (25–30 km).


## Introduction and objectives

Raw material procurement constitutes the first phase of any lithic production *chaîne opératoire* (Leroi-Gourhan 1964; Geneste 1985; Soressi and Geneste 2011) as the practical execution of an explicit project's conceptual framework. Nowadays, the study of raw material origin and circulation —alongside techno-morphological characterisation, functional analysis, and the resulting economic and subsistence inferences— represents an essential research process for interpreting Palaeolithic contexts, as they reflect the behaviour of human communities (Fernandes et al. 2008; Browne and Wilson 2011).

Diachronic research examining the intrinsic properties of lithic raw materials has underscored their critical role in modulating technocomplex variability and expression (Goodman 1944; Rolland and Dibble 1990; Dibble 1991). Specifically, these parameters are fundamental to elucidate spatial and mobility implications (Ambrose and Lorenz 1990; Geneste 1991; Kuhn 1991, 2020; Brantingham 2006); occupational patterns, duration, and seasonality (Feblot-Augustins 1993, 1999; Kuhn 2004); techno-morphological and techno-economic dynamics (Straus 1991; Eixea et al. 2014; Villeneuve et al. 2019; Melo et al. 2025); as well as social (Renfrew 1984) and subsistence connotations (Moncel et al. 2014), among others. Consequently, sourcing raw materials must not be considered an ultimate objective, but rather a preliminary baseline to decipher the underlying mechanisms of resource selection, landscape constraints, topographic friction, and human energy costs (Wilson 2007).

These analyses are executed via the systematic and independent characterisation of the respective geological and archaeological raw materials, establishing subsequent petrographic correlations between both sample sets. This methodological approach enables the identification of source areas for the materials recovered at the site, distinguishing between local and non-local resources, while charting their spatiotemporal distribution across successive occupational phases (Belmiro et al. 2025). For instance, in the Vaucluse region of southern France, Browne and Wilson (2011) deployed multi-variable models to assess the costs and benefits associated with the exploitation of potential raw material sources, subsequently benchmarking these predictive models against the lithic assemblages from the Middle Palaeolithic site of Bau de l'Aubesier. Similarly, the Iberian Peninsula offers a robust body of literature that clarifies how distinct prehistoric communities managed available lithic resources (Aubry et al. 2016; Gómez de Soler et al. 2020; García-Rojas et al. 2021; Costa et al. 2022; Sánchez de la Torre et al. 2023).

The presence or absence of specific raw materials within Palaeolithic sites may be linked to direct procurement from relatively proximal source areas, exploitation of more distant outcrops, or even inter-community exchange networks (Kelly 1983; Gamble

1999; Burke 2012). In this regard, lithic provenance studies of European Middle Palaeolithic assemblages have conventionally confirmed that Neanderthals procured raw materials for tool manufacture mainly from local or semi-local supply areas (Geneste 1988; Roebroeks 1988; Féblot-Augustins 1999). Nevertheless, compelling evidence from specific Mousterian assemblages also supports the existence of long-distance procurement strategies (Slimak and Giraud 2007).

Geneste (1985) introduced an economic zoning framework designed to classify distinct raw material procurement strategies. This model correlates the distance between an archaeological site and its raw material sources with the corresponding energy costs. To this end, he proposed three micro-regional procurement zones defined by precise distance thresholds (< 5 km, 5–20 km, and 20–80 km); with minor adaptations, this spatial classification continues to offer a primary reference frame for contemporary lithic studies (Abrunhosa 2020).

Lithic procurement patterns documented for the Middle Pleistocene show that resources obtained between 30 and 100 km from a site are sparse within archaeological assemblages. Indeed, the overwhelming majority of lithic materials originate either from immediate sources (within a < 5 km local foraging radius) or from intermediate localities situated between 5 and 20 km (Fernandes et al. 2008).

Another key axis of debate focuses on the geological nature of procurement contexts, specifically distinguishing between primary and secondary sources. This classification hinges on whether raw materials were acquired directly from *in situ* bedrock formations at geological outcrops (Baena et al. 2011; Prieto et al. 2019) or from redeposited contexts within fluvial or colluvial formations, with the latter being the most frequently exploited source type (Fernandes and Raynal 2007; Fernandes et al. 2008).

Palaeolithic human groups exploited a wide array of lithic raw materials, the selection of which—according to well-established literature—was modulated by diverse criteria, including availability, accessibility, mechanical quality, morphology, blank dimensions, aesthetic attributes, or cultural traditions. Recently, a novel selective criterion has been proposed, based on the implementation of lithic strategies linked directly to site functionality; in the specific case of the Gran Dolina TD10.2-BB sublevel, this is evidenced by its role as a specialised butchering and processing site (Arteaga-Brieba et al. 2026).

In any case, the most common and recurrent lithologies exploited in Western Europe have been non-detrital sedimentary siliceous rocks, commonly referred to as flint (chert), which are highly prized for their excellent knapping properties, along with quartzite and other materials to a lesser extent. Among the latter, quartz has traditionally been considered an alternative and secondary resource when the surrounding environment lacked high-quality raw materials (cryptocrystalline rocks) (Mourre 1996); this is due to its fracture mechanics, which cause quartz artifacts to deviate from the descriptive and interpretive standards established for higher-quality knapping materials (Lombera-Hermida et al. 2011).

Nevertheless, numerous procurement studies focusing on Western European Middle Palaeolithic assemblages have emphasised the predominance of local raw materials, such as quartz, over non-local resources. Notable examples include Calvero de la Higuera (Abrunhosa 2019), Cueva de Teixoneres (Pincin et al. 2020, Uzudinis et al. 2024), Jarama VI (Navazo et al. 2020), Maltravieso (Peña 2008), Cova Eirós (De Lombera-Hermida et al. 2021), Figueira Brava (Melo 2025), and Cardina-Salto do Boi (Aubry et al. 2022).

At the La Sima Cave, the knapping products were manufactured predominantly from quartz, supplemented by a minor component of quartzite, flint, and other lithic materials. Overall, this significant MIS-3 lithic assemblage (ca. 40–50 ka) provides the baseline to establish the primary objective of this study: to determine the exploited lithic raw material sources in order to reconstruct Neanderthal territoriality and subsistence strategies during the Middle Palaeolithic within the region.

## La Sima Cave: archaeological background

La Sima Cave is an archaeological site located on the southwestern periphery of the Constantina municipality (Seville, Spain), within the Sierra Norte de Sevilla UNESCO Global Geopark (Fig. 1). Known since the mid-20th century, this subterranean cavity has undergone several intervention phases that have shaped its current state of preservation (Carriazo 1974; Rodríguez et al. 2003; Álvarez et al. 2005; Caro et al. 2013, 2017, 2026; Riquelme et al. 2025). However, it is over the last decade—with the implementation of the CAREQ general research project—that the site has revealed the true significance of its archaeological

record. The upper stratigraphic levels, dating to the Mid-Holocene (ca. 4,000 BP), document the use of the cave as a burial ground during the Chalcolithic, although these deposits are unfortunately highly disturbed (Caro et al. 2017). Conversely, the lower stratigraphic units have yielded an abundant lithic industry attributable to Middle Palaeolithic technocomplexes, found in close association with rich macrofaunal assemblages including aurochs, rhinoceros, horse, bear, lynx, and hyena, among others.

During this period, several excavation campaigns have been carried out in the so-called Galería Antigua, establishing a stratigraphic sequence where six Geoarchaeological Units (GAUs) have been identified (Riquelme et al. 2025; Caro et al. 2026). Among these, the uppermost units (GAU 1 and GAU 2) consist of modern ditch infills resulting from interventions conducted in the 1950s (Caro et al. 2013), whereas the remaining units (GAU s 3, 4, 5, and 6) constitute the Pleistocene sedimentary record.

Excavations carried out in these Pleistocene deposits (GAU 4, GAU 5, and GAU 6) have yielded 1,810 lithic artifacts, which are considered as a single assemblage for techno-morphological characterization (Caro et al. 2026). Regarding lithology, the collection is dominated by quartz (1,564 pieces; 86.4% of the total), supplemented by quartzite (166 pieces; 9.2%), flint (67 pieces; 3.7%), and other raw materials (13 pieces; 0.7%).

The technological analysis of the assemblage reveals that debris is the most representative category (32.4%), followed by debitage (23.1%), and, in very similar proportions, flakes and cores (19.6% and 20.4%, respectively), alongside a small group of retouched tools (1.4%). To these must be added a set of poor-quality quartz nodules that show no knapping stigmata (3.1%) but must have been intentionally introduced into the deposits.

From a chronological perspective, previous work established an age of 72,500 ± 3,000 BP (U/Th) for the lower part of GAU 6 (Rodríguez-Vidal et al. 2003). During the development of the CAREQ research project, radiocarbon (14C AMS) and uranium-series (U/Th) analyses conducted on charcoal fragments from GAU 5 established chronologies ranging from 50,500 ± 2,200 BP at the base to 40,600 ± 1,100 BP at the top. Similarly, above the flowstone separating UGA 4 from GAU 3, a bear tusk yielded a (U/Th) age of 20,473 + 3,691/-3,587 BP (Riquelme et al. 2025; Caro et al. 2026). This flowstone was dated in previous studies (Rodríguez-Vidal et al. 2003), yielding two chronologies: one at the top (26.3 ± 2.5 ka Th/U) and another at the base (43.8 ± 3.8 ka Th/U). Finally, recently analysed charcoal samples from GAU 3 span a narrow chronological window of 80 years, ranging between 12,270 ± 40 BP and 12,190 ± 40 BP (mean radiocarbon age) (Riquelme et al. 2025; Caro et al. 2026).

## Materials and methods

The materials analysed in this study originate from the successive excavations carried out in the Galería Antigua of La Sima Cave. The entire assemblage was examined following a techno-typological approach aimed at identifying the different production phases and technical criteria described within the framework of the *chaîne opératoire* (Lemonnier 1976, 1986; Karlin et al. 1991; Caro et al. 2023).

The lithological singularity of the recovered assemblage—predominantly developed on quartz blanks—alongside the lack of regional studies on this specific raw material, prompted us to undertake a characterisation analysis on a representative sample of lithic pieces. For the material selection, an initial classification of the different exploited quartz varieties was conducted across the site's various GAUs, based on macroscopic criteria such as grain size, colour, and fracture quality.

Conversely, the location of quartz outcrops potentially exploited during Middle Palaeolithic was approached using a two-phase methodology. First, a preliminary planning phase was conducted based on the lithological analysis of the surroundings, utilizing the geological mapping provided by the Geological and Mining Institute of Spain (IGME). Once the geological map had been studied and potential host formations for these materials were identified, several field survey campaigns were carried out. These covered a radius vector of approximately 25 km to the south—the distance separating the site from the Guadalquivir River terraces —and slightly less (15 km) towards the remaining cardinal points, encompassing a total area of approximately 1,000 km².

This fieldwork enabled the location of several quartz outcrops containing the varieties macroscopically recognized *de visu* within a significant portion of the archaeological material, allowing us to establish an initial geological characterisation of the area. Additionally, several watercourses (rivers and streams) that affected these outcrops by eroding and transporting the materials were surveyed, such as the Guadalbacar Stream, which flows southward from the vicinity of the site until it drains into the Guadalquivir River.

A spatial approach based on Geographic Information Systems (GIS), using QGIS software version 3.42.1, was used during the study. This tool allowed the integration and management of spatial information regarding the surroundings of La Sima Cave, facilitating the analysis of quartz outcrops by combining topographic, hydrographic, and geological data. GIS processes included viewshed analysis of the landscape, the calculation of least-cost paths, resource catchment analysis, and the calculation of accumulated travel costs, aimed at understanding the relative accessibility and complexity of the environment.

Data processing began with the collection of cartographic information from institutional sources, such as the Instituto Geográfico Nacional (IGN). Based on this dataset, a Digital Terrain Model (DTM) with a 5-metre cell resolution was generated, derived from LiDAR data available through the Centro Nacional de Información Geográfica (CNIG), into which a vector layer corresponding to the hydrographic network (rivers) was integrated. This DTM served as the baseline to generate other models using GRASS tools, such as *r.slope.aspect* to estimate the slope of the DTM and to obtain friction and viewshed models.

For the viewshed analysis, the *r.viewshed* tool was used to define the visible area from the site, taking into account the curvature of the Earth's surface and the average height of a human observer (estimated at 1.70 metres). This is crucial for determining the degree of visual control from this Mousterian site over the immediate territory (Wheatley and Gillings 2002).

The mobility and route analysis was developed using an accumulated cost model, executed with the GRASS tool *r.cost*. This enabled the generation of a cost surface map from the DTM, simulating the relative effort required to move across the topography while considering slope values and other potential natural obstacles.

Based on the slope model, the least-cost paths were calculated from the site to the previously georeferenced quartz outcrops using the cost distance analysis function: Least Cost Path (LCP). This approach allows the most efficient route to approximate the actual energy expenditure associated with human movement across mountainous terrain (Tobler 1993; Wheatley and Gillings 2002; Verhagen et al. 2014).

Finally, to delimit the resource catchment area, a human travel threshold equivalent to a 120-minute walk was established. This parameter follows the mobility models for hunter-gatherer groups (Vita-Finzi and Higgs 1970), with the reclassification of the cost map using the GRASS tool *r.reclass*. This operation enabled the identification of the accessible boundaries of the territory from the site, thereby defining an isochrone that delineates the area available for raw material procurement.

In addition, based on the sampling of various quartz outcrops in the surroundings and the selection of knapped quartz lithic artefacts from the cave, a petrological analysis—including thin sections and X-ray fluorescence (XRF)—was conducted to identify the characteristics and variability of the quartz, as well as the similarities and/or differences between both datasets. Finally, a statistical analysis was applied for data processing, organisation, and interpretation.

Petrographic analysis was conducted on 24 thin sections of massive quartz bodies from two sampling series. These were divided into two main groups based on their origin: natural outcrops (coded as CZno.) or archaeological deposits (lithic industries, coded as SIM). Furthermore, macroscopic characterisation allowed for the differentiation of distinct varieties within some of these outcrops (coded as CZno.-no. …) (Table 1) (Figs. S1 to S8).

Table 1
Designation of the samples examined in the petrological analysis.

| **Outcrops** | **Group** | **Samples** |
|---|---|---|
| Tierras Nuevas | CZ1 | CZ1-1, CZ1-2, CZ1-3, CZ1-4 |
| Las Majadillas | CZ2 | CZ2-1, CZ2-2 |
| Malpicas | CZ3 | CZ3-1, CZ3-2, CZ3-3 |
| Sierra de Los Ganazos | CZ4 | CZ4-2 |
| Castillo de Setefilla | CZ5 | CZ5-1 |
| **Site** | **GAUs** | **Samples** |
| Lithic artefact | GAU4 | SIM.22–170 |
| Lithic artefact | GAU4 | SIM.22–801 |
| Lithic artefact | GAU5 | SIM.22–82 |
| Lithic artefact | GAU5 | SIM.22–133 |
| Lithic artefact | GAU5 | SIM.22–175 |
| Lithic artefact | GAU5 | SIM.22–246 |
| Lithic artefact | GAU5 | SIM.22–611 |
| Lithic artefact | GAU5 | SIM.22–856 |
| Lithic artefact | GAU5 | SIM.22–865 |
| Lithic artefact | GAU6 | SIM.22–520 |
| Lithic artefact | GAU6 | SIM.22–322 |
| Lithic artefact | GAU6 | SIM.22–365 |
| Lithic artefact | GAU6 | SIM.22–520 |

Observations were performed using a Nikon LV100ND petrographic microscope under plane-polarised light (PPL) and cross-polarised light (XPL), at magnifications of 2x and 4x.

The elemental composition of the samples was determined by wavelength dispersive X-ray fluorescence (WDXRF) using a Rigaku ZSX Primus IV spectrometer equipped with a 4 kW Rh X-ray tube. This type of equipment allows for the determination of elements from Be to U in solid, powder, or fused bead samples with high spectral resolution (Potts et al. 1985). This technique represents a well-established tool in archaeometry for the elemental characterisation of geological materials and archaeological artefacts (Shackley 2020). Two types of samples were selected for the geochemical analysis: geological samples from the quartz outcrops, and lithic artefacts recovered during the archaeological excavations (Table 2). This comparative methodological design allows for the contrast of the elemental composition of the artefacts with that of potential geological sources—a strategy widely utilised in provenance studies of lithic raw materials and other archaeological findings (Forster et al. 2011; Frahm 2013).

To ensure the reliability of the findings, this study was combined with multivariate statistical methods developed entirely within the R environment (v.4.3.0), following an explicitly reproducible workflow. The geochemical data (XRF) from 13 samples—comprising 4 geological sources (CZ) and 9 archaeological artefacts (SIM)—were processed by omitting $CO_2$ (balance) values (Table 2). Three analytical visualisations were generated:

1) Faceted boxplots. To explore the distribution of each element by sample type (source vs. artefact), boxplots were built using independent facets, free Y-axis scales, and a pseudo-logarithmic transformation to accommodate zero values. Semi-transparent jittered points were overlaid to display the actual dispersion of the data.

2) Principal Component Analysis (PCA). Prior to data standardisation and the verification of the suitability of the correlation matrix via Bartlett's Test of Sphericity ($p < 0.001$), a PCA was applied. The resulting biplot displayed the sample scores—labelled using the *ggrepel* repulsion algorithm to avoid overlaps—and the variable loadings as arrows, which indicate the direction and contribution of each element to the first two principal components (PC1: 32.9%, PC2: 25.1%).

3) Minimum distance assignment and arrow map. To determine the most probable source of origin, Euclidean distances were calculated within the space of the first five principal components (which explain 88.5% of the variance). Each artefact was assigned to the source with the minimum distance. Arrows connecting each artefact to its assigned source were drawn on the PC1–PC2 plane, applying the colour of the corresponding source. For those with at least three samples, 95% confidence ellipses illustrating their internal variability were added (although no source met this criterion).

Table 2
Designations of the samples analysed in the geochemical analyses.

| **Outcrops** | **Group** | **Samples** |
|---|---|---|
| Tierras Nuevas | CZ1 | CZ1-1, CZ1-3 |
| Las Majadillas | CZ2 | CZ2-1 |
| Malpicas | CZ3 | CZ3-2 |
| **Site** | **UGAs** | **Samples** |
| Lithic artefact | GAU4 | SIM-21.126 |
| Lithic artefact | GAU4 | SIM-21.134 |
| Lithic artefact | GAU5 | SIM.22–619. AA7 |
| Lithic artefact | GAU5 | SIM.22–744. AA7 |
| Lithic artefact | GAU5 | SIM.22–863. A6 |
| Lithic artefact | GAU5 | SIM-22.362 |
| Lithic artefact | GAU5 | SIM-22.719 |
| Lithic artefact | GAU6 | SIM-22.753 |
| Lithic artefact | GAU6 | SIM-22.590 |

## Results

# Archaeological surveys for lithic raw material sourcing

As previously noted, the three primary raw materials used for knapping at La Sima Cave are quartz, quartzite, and chert, in that order of importance, with an absolute dominance of the former. Locating the catchment areas for each of these raw materials is essential for understanding the behaviour of the human groups that exploited them. To this end, numerous fieldwork surveys and territorial analyses were implemented, backed by our pre-existing regional expertise gained through decades of continuous research in the area (Díaz del Olmo et al. 2023).

One of these studies focused on the Guadalquivir River terraces in the Carmona sector, where the lithological characterisation of the alluvial cobbles arranged them into three siliciclastic assemblages, dominated by a group of quartzites (50.79%), quartz (24.89%), quartzitic sandstone (8.86%), and sandstone (8.82%) (Caro et al. 2011). Within the quartzite cobbles, two types of petrographic microfabrics have been identified: fine-grained quartzites and fine-grained quartzites with quartz phenocrysts and diverse mineral inclusions. The former offers the highest quality for lithic knapping and was also the most frequently exploited, although it is not the only one present in many of the Palaeolithic series within the general Guadalquivir sequence (Caro et al. 2026).

Meanwhile, quartzite elements from La Sima Cave correspond to the characteristics of the first type described, which allows these alluvial deposits to be identified as a procurement source for this lithology. Additionally, it has been verified that a selective sorting process must have taken place at the source to select those cobbles with the most suitable qualities for knapping. A similar pattern is observed for the few recovered chert artefacts, whose macroscopic characterisation matches—although not in all cases—the varieties detected in the Guadalquivir terraces, where they represent a minority lithofacies (1.8%).

Having clarified the source of the minority raw materials (quartzite and chert) within La Sima Cave lithic assemblages, it was necessary to elucidate the potential source areas for quartz, the predominant raw material in these series. The archaeological surveys conducted led to the localisation of several primary sites featuring quartz vein outcrops, alongside other nearby locations with accumulations of cobbles transported by the eroding local streams and rivers (Figs. 2 and 3).

## Procurement routes and accessibility (least-cost path analysis)

Spatial analyses aimed to comprehend the accessibility and potential exploitation of the quartz outcrops and Guadalquivir terraces from La Sima Cave, factoring in variables such as optimal routes (Fig. 3), cumulative travel cost, viewsheds, and procurement areas.

The least-cost path analysis identifies the trajectories presenting the lowest friction and geographical difficulty between La Sima Cave and the various outcrops. These routes primarily traverse small, incised valleys and moderate slopes, effectively bypassing steep terrain. Furthermore, certain pathways tend to track fluvial courses, such as the Hueznar River and the Guadalbacar Stream. This suggests that rivers served a double purpose: they were not only crucial resource cores but may also have functioned as natural mobility corridors, facilitating movement across the wider landscape towards areas like the Guadalquivir River terraces. Notably, both fluvial courses connect to this main river, and one of the quartz outcrops (Castillo de Setefilla) is located near the confluence of the Guadalbacar Stream and the Guadalquivir River, reinforcing the hypothesis of a mobility strategy structured around these hydrographic networks.

Viewshed analysis from the site identifies the landscape areas visible from the cave itself (Fig. 4), with zones under direct line-of-sight highlighted in red. The results demonstrate that the site has a restricted field of view, constrained by the surrounding topography, which limits direct observation of several nearby outcrops. Nevertheless, there is clear visibility towards a section of the route leading to the Malpicas outcrop (CZ3). Given that samples from this source appear to be among the most profoundly employed, visibility in this case may have been a significant factor in both resource foraging and territorial surveillance (Wheatley and Gillings 2002).

The cumulative travel cost map (Fig. 4) displays the energy or physical effort required for an individual to move from the site to any point within the landscape, accounting for local geographical features. The lowest cost values (blue hues) indicate areas of higher accessibility and ease of movement, whereas high-cost values (reddish hues) correspond to challenging terrain, typically due to steep slopes. Data show that travel cost increases progressively with distance from the site or when crossing rugged topography.

Furthermore, the routes towards the several outcrops clearly follow low-cost gradients, validating the energy efficiency of the identified trajectories. However, two exceptions with moderate accessibility are identified: Sierra de los Ganazos and Castillo de Setefilla, both of whose pathways present greater geographical complexity.

In addition, catchment area analysis defines the zones accessible from the site within specific travel-time intervals (Fig. 4):

- 30-minute zone: involves the immediate procurement area, covering a limited surface around the site. The cave itself is located within this band, although its quartz is of a very poor quality.
- 60-minute zone: extends the foraging area, within whose boundaries no potential quartz sources have been located.
- 120-minute zone: covers the maximum extent of the procurement area, granting access to most outcrops, including Tierras Nuevas and Malpicas, whereas Las Majadillas is situated on the threshold, slightly beyond this range. Meanwhile, the Sierra de los Ganazos and Castillo de Setefilla outcrops lie well past this limit; although a trip to these areas could be achieved within a single day, they appear too distant to be considered part of a daily foraging range

## Petrological characterisation of quartz

In general terms, the analysed samples consist of quartz aggregates, which is the primary component. They exhibit an inequigranular mosaic granoblastic texture, though a bimodal grain-size distribution typical of porphyroblastic texture is occasionally observed. Quartz grains display undulose extinction of varying intensity, indicative of mechanical deformation. Microfractures are common, with rectilinear and curvilinear fissures, alongside internal veins filled with microcrystalline quartz with an average size of 55 μm (ranging between 20 and 80 μm).

Feldspars and micas (sericite being the most common) were identified as accessory minerals, alongside occasional metallic ores (possibly haematite), specifically within sample CZ1-4.

# By outcrop groups

CZ1 Series (Tierras Nuevas). Samples CZ1-1 to CZ1-3 exhibit an inequigranular granoblastic texture, with medium- to coarse-grained crystals. Intergranular contacts are predominantly straight to slightly sutured. They present moderate undulose extinction and scattered microfractures with no significant filling. Sample CZ1-4 is distinct from both the rest of the series and the overall sample assemblage; it features a fine- to medium-grained granoblastic texture, with a grain-size distribution ranging from 65 to 220 μm and an average size of 118 μm, predominantly clustering within the 90 to 100 μm range.

CZ2 Series (Las Majadillas). Samples from this series (CZ2-1, CZ2-2) exhibit a homogeneous, medium-grained granoblastic texture, with straight to slightly curved contacts, weak undulose extinction, and a high density of microfractures and internal veins.

CZ3 Series (Malpicas) (CZ3-1, CZ3-2, CZ3-3). Sample CZ3-2 displays areas with sutured contacts and more irregular grain sizes, whereas CZ3-3 features more intense microfracturing. In both samples, fine quartz veins associated with microfissure filling or mechanical deformation can be distinguished.

CZ4 Series (Sierra de Los Ganazos) (CZ4-1 and CZ4-2). Sample CZ4-2 unveils porphyroblastic texture and notable, yet sparse, microfracturing. Overall, samples from this series present the most sutured contacts.

CZ5 Series (Castillo de Setefilla). Sample CZ5-1 corresponds to the general description of the sample assemblage, showing no significant alterations or differences.

## Archaeological lithic artefacts

Overall, the SIM Series samples (SIM-82, 133, 170, 175, 246, 322, 365, 520, 611, 801, 856, 865) are characterised by a highly homogeneous petrographic profile, defined by a medium-grained, inequigranular granoblastic texture with variable undulose extinction and common microfracturing. Fine quartz veins, nonetheless, occur with greater frequency in SIM-246, SIM-365, and SIM-801.

## X-ray fluorescence (XRF) and statistical analysis

X-ray fluorescence (XRF) geochemical analysis, applied to both geological samples from quartz outcrops and lithic artefacts from the archaeological excavation, yielded the following results (Table 3):

Table 3
XRF geochemical analysis of quartz samples from La Sima Cave.

| Sample | Na | Mg | Al | Si | P | S | Cl | K | Ca | Ti |
|---|---|---|---|---|---|---|---|---|---|---|
| **CZ1-1** | 0.295 | 0.234 | 5.36 | 19.5 | 0.0584 | 0.0382 | 0.286 | 0.575 | 0.0765 | 0.0489 |
| **CZ1-3** | 0.135 | 0.213 | 2.95 | 24.3 | 0.0632 | 0.0195 | 0.0526 | 0.796 | 0.0676 | 0.0393 |
| **CZ2-1** | 0.0536 | 0.0315 | 0.285 | 34.6 | 0.012 | 0.0106 | 0.459 | 0.0295 | 0.0217 | 0 |
| **CZ3-2** | 0.105 | 0.199 | 2.93 | 73.4 | 0.0153 | 0.017 | 0.106 | 0.126 | 0.0399 | 0 |
| **SIM.22–619** | 0.19 | 0.0754 | 0.837 | 30.4 | 0.0272 | 0.0162 | 0.133 | 0.167 | 0.0405 | 0 |
| **SIM.22–744** | 0 | 0 | 0.239 | 33.9 | 0.035 | 0.0000872 | 0.0204 | 0.114 | 0.967 | 0 |
| **SIM.22–863** | 0.0325 | 0.0121 | 0.167 | 29.5 | 0.371 | 0.0000839 | 0.0341 | 0.0457 | 0.35 | 0 |
| **SIM-21.126** | 0.297 | 0.146 | 1.07 | 63.5 | 0.283 | 0.122 | 0.147 | 0.185 | 1.97 | 0 |
| **SIM-21.134** | 0 | 0.072 | 0.566 | 57.8 | 0.0478 | 0.0156 | 0.0167 | 0.0746 | 0.745 | 0 |
| **SIM-22.362** | 0.0466 | 0.245 | 4.28 | 56.7 | 0.113 | 0.0241 | 0.0214 | 0.248 | 0.531 | 0 |
| **SIM-22.590** | 0.0365 | 0.051 | 0.658 | 81.1 | 0.044 | 0.0303 | 0 | 0.0793 | 0.134 | 0 |
| **SIM-22.719** | 0 | 0.127 | 1.23 | 60 | 0.168 | 0.029 | 0 | 0.211 | 0.706 | 0 |
| **SIM-22.753** | 0 | 0.102 | 0.919 | 69 | 0.0831 | 0.0286 | 0.0388 | 0.113 | 1.41 | 0 |

Table 3
XRF geochemical analysis of quartz samples from La Sima Cave (continuation).

| Sample | Mn | Fe | Ni | Cu | Zn | As | Sr | Ba | CO2 |
|---|---|---|---|---|---|---|---|---|---|
| **CZ1-1** | 0.0000759 | 0.738 | 0.00000892 | 0 | 0.0000248 | 0 | 0.00000884 | 0.0271 | 72.7 |
| **CZ1-3** | 0.0000993 | 0.618 | 0 | 0 | 0.0000158 | 0 | 0 | 0 | 70.8 |
| **CZ2-1** | 0 | 0.0309 | 0 | 0 | 0 | 0 | 0 | 0 | 64.9 |
| **CZ3-2** | 0 | 0.0558 | 0 | 0 | 0 | 0 | 0.0000145 | 0 | 23 |
| **SIM.22–619** | 0.0000334 | 0.0894 | 0.0000209 | 0.0000214 | 0.00000980 | 0 | 0 | 0 | 68.1 |
| **SIM.22–744** | 0 | 0.065 | 0.0000191 | 0 | 0 | 0 | 0 | 0 | 64.7 |
| **SIM.22–863** | 0 | 0.0254 | 0 | 0 | 0 | 0.00000732 | 0.0000154 | 0.0155 | 69.4 |
| **SIM-21.126** | 0 | 0.561 | 0 | 0 | 0.0221 | 0 | 0.0000244 | 0 | 31.7 |
| **SIM-21.134** | 0 | 0.0663 | 0 | 0 | 0 | 0 | 0 | 0 | 40.6 |
| **SIM-22.362** | 0 | 0.56 | 0 | 0 | 0.0000419 | 0 | 0.0000189 | 0 | 37.2 |
| **SIM-22.590** | 0 | 0.104 | 0 | 0 | 0 | 0 | 0 | 0 | 17.9 |
| **SIM-22.719** | 0 | 0.137 | 0 | 0 | 0.0000293 | 0 | 0 | 0 | 37.4 |
| **SIM-22.753** | 0 | 0.106 | 0 | 0 | 0 | 0 | 0 | 0 | 28.2 |

The obtained results are consistent with the nature of the analysed samples: quartz, a mineral composed of silicon dioxide ($SiO_2$). Consequently, Si is invariably the dominant element, with values ranging between 19.5% and 81.1%.

This elemental quantification analysis was combined with multivariate statistical methods to establish provenance links between the archaeological artefacts and their potential source areas.

The geochemical characterisation of the samples was approached through exploratory and multivariate analyses to assess the compositional affinity between the source areas (CZ) and the archaeological artefacts (SIM). Faceted boxplots allowed for the visual inspection of the independent distribution of each chemical element, thereby avoiding the compression effect caused by differing scales of magnitude (Fig. 5). Furthermore, the applied pseudo-logarithmic transformation facilitated the representation of values near the detection limit without distorting the distributions.

The results reveal a highly pronounced enrichment in phosphorus (P) and calcium (Ca) within the archaeological artefacts compared to the source samples. While concentrations in the latter are virtually negligible, the artefacts reach values of up to 0.37% P and 1.97% Ca. This pattern is consistent with post-depositional contamination processes associated with the incorporation of organic materials, such as bone remains, ashes, or excrement, during the occupation of the site.

Silicon (Si), the dominant element across all samples, constitutes the primary factor for lithological differentiation among the sources. CZ3-2 and CZ2-1 exhibit the highest Si contents (> 70% and > 60%, respectively), whereas CZ1-1 and CZ1-3 show distinctly lower values. The archaeological artefacts are mostly distributed within these ranges, with a trend towards high Si contents observed in samples subsequently assigned to CZ3-2. Conversely, aluminium (Al) and iron (Fe) primarily discriminate sources CZ1-1 and CZ1-3, which are characterised by higher concentrations of both elements. Certain artefacts, particularly SIM.21–134 and SIM.22–362, present relatively elevated Al and Fe values and occupy intermediate positions relative to the known sources, suggesting the potential existence of an additional unsampled source. Trace elements (Mn, Ni, Cu, Zn, As, Sr, and Ba) display generally low concentrations and a limited contribution to group discrimination.

A Principal Component Analysis (PCA) was performed on the previously standardised elemental concentrations with the objective of integrating the multivariate structure of the geochemical dataset (Fig. 6). Bartlett's test of sphericity validated the suitability of this analysis ($\chi^2=487.3$; $p < 0.001$). The first two principal components jointly account for 58.0% of the total variance (PC1 = 32.9%; PC2 = 25.1%), a percentage sufficient to visualise the main compositional trends.

The PCA biplot demonstrates a clear separation among the geological sources. Sample CZ3-2 dominates the upper-right quadrant and is primarily associated with high Si contents, whereas CZ1-1 and CZ1-3 are positioned in the lower part of the plot, controlled by higher concentrations of Al, Fe, K, and Ti. Meanwhile, sample CZ2-1 is in an intermediate position, discriminated from both the siliceous sources and those enriched in Al-Fe.

The archaeological artefacts cluster into two main trends. A first group, including SIM.22–619, SIM.22–744, and SIM.22–863, shows an affinity with CZ2-1. A second group, consisting of SIM-21.126, SIM-22.590, SIM-22.719, and SIM-22.753, plots within the vicinity of CZ3-2. Samples SIM-21.134 and SIM-22.362 present intermediate positions, shifted towards the compositional domain of CZ1, although they do not fully overlap with any of the analysed sources.

The loading analysis confirms that silicon is primarily responsible for the positive differentiation along PC1, whereas Al, Fe, K, and Ti control the negative values of PC2. Meanwhile, P and Ca exhibit independent orientations, reflecting specific post-depositional processes rather than primary lithological differences.

Finally, to determine the most feasible source of each archaeological artefact, an assignment procedure was applied based on Euclidean distances calculated over the first five principal components, which retain 88.5% of the total variance (Fig. 7). The results demonstrate high consistency with the structure observed in the PCA. Artefacts SIM.22–619 and SIM.22–863 were assigned to CZ2-1, whereas the majority of the remaining archaeological samples are linked to CZ3-2. Among the latter, SIM-22.590, SIM-22.719, and SIM-22.753 stand out, unveiling the shortest distances to this source and, therefore, the highest compositional similarity.

Artefact SIM.22–744 is the only partially discordant case, given that, despite its visual proximity to CZ2-1 on the PC1–PC2 plane, it was ultimately assigned to CZ3-2 when the higher-order components of the PCA were considered. This behaviour reflects the influence of its high P and Ca contents on the higher-order multivariate dimensions. Samples SIM-21.134 and SIM-22.362, although likewise assigned to CZ3-2, maintain intermediate positions and partially differentiated compositions, thereby reinforcing the hypothesis of a greater diversity of procurement sources, or varieties within the sources, than currently documented.

## Discussion and Conclusions

Throughout the results, it has been validated that the primary raw material exploited in the production of the lithic industry at La Sima Cave is quartz (Fig. 8. 1,2,3,4,5), in its diverse forms. This material consistently exhibits a local origin, as all main procurement sources are located within a 15 km radius (Geneste 1991; Kuhn 2020), with a clear preference for the exploitation of nearby resources. Consequently, the most frequently used varieties are predominantly related to several samples from the CZ2 and CZ3 series, and even to CZ1. Visual inspection reveals that all samples exhibit macroscopic features consistent with the milky and translucent quartz varieties documented at the Maltravieso and Cueva de Santa Ana sites (Peña 2008). Furthermore, they can be classified within some of the varieties described at Cardina-Salto do Boi (Guarda, Portugal), such as J8 (Anhedral glossy white quartz), J9 (Anhedral milky and grey quartz), and J11 (Anhedral zoned translucent to clear quartz) (Aubry et al. 2022).

However, there is also a significant percentage of quartzite artefacts that, through macroscopic identification, have been predominantly assimilated to the type containing fine quartz grains, which offers the highest quality for knapping (Fig. 8.6,7,8,9). Future research using new petrogenetic procedures will allow for a more precise characterisation and a more refined identification. This will enable the establishment of reliable and universal types that facilitate the understanding of quartzite from a geoarchaeological perspective (Prieto et al., 2026). In any case, their provenance, which has been documented in the alluvial deposits of the Guadalquivir River (~ 30 km away), alongside the use of flint (Fig. 8.10,11,12,13), indicates a clear concern for obtaining higher-quality materials; at certain times, this would compel them to move beyond the immediate catchment area for their procurement. It is commonly observed that these higher-quality raw materials are employed to develop more complex *chaînes opératoires*, such as Levallois or discoidal debitage, a behaviour well-documented in the European Middle Palaeolithic (Geneste 1996). Particularly in relation to the different SU (Stratigraphic Units) analysed, a certain increase in the use of quartzite and flint is observed in SU 5, contrasted with an almost exclusive reliance on quartz in SU 6.

In this regard, the high fragmentation of reduction sequences and the presence of shaped tools introduced into the site, which refer to non-local raw materials, provide evidence of advanced planning; this was likely triggered by the inherent limitations of the autochthonous raw materials (Kuhn 1995) and the technological requirements for producing elements of greater technical complexity.

At Cardina-Salto do Boi, within the chronologically similar levels to La Sima Cave—dated to 51 ka and 39 ka, attributable to the Late Middle Palaeolithic—all exploited raw materials are of local origin, available near or a few kilometres from the site. Among them, the most frequently exploited lithology was quartz, which, unlike at La Sima, was frequently used to obtain products through discoidal and prismatic reduction strategies. Similar strategies have been reported at French sites such as Abri du Maras, Payre, or Abri des Pêcheurs, featuring chronologies similar to La Sima (MIS 4 – 3), whose records suggest brief and recurrent bivouac-type occupations (Moncel et al. 2008). Just as in La Sima Cave, these sites predominantly contain flakes and some cores, including the use of local quartz, but also a diverse range of other raw materials from alluvial and colluvial deposits, collected within a wide perimeter of 10 to 30 km (Moncel et al. 2021).

The technological structure of the La Sima Cave lithic assemblage displays an equilibrium that we consider well-balanced for the quartz series (a ratio of 5 artefacts per core); however, the absence of quartzite and flint core-like elements results in a highly fragmented reduction sequence in both cases, leading to a total lack of balance (Caro et al. 2026). Although the entire potential surface area of the cavity that could host these materials has not been fully excavated, the most probable reason is likely related to the greater distance to the procurement sources of these raw materials, which led to the transport of already manufactured products to the site.

A predominance of unidirectional, bidirectional, and polyhedral reduction strategies has been defined at La Sima Cave, likely relating to a methodological response adapted to the morphology and fracturing properties of the predominantly utilised quartz

blanks (Caro et al. 2026). However, cores involving more elaborate technical processes, such as centripetal, Levallois, or Kombewa methods, are restricted to the use of other higher-quality lithologies (flint and quartzite). In this regard, Andrefsky (1994) proposes that a correlation exists between the technologies and the quality and abundance of the raw material; thus, when using low-quality raw material, the technologies tend to be modified and become less formal due to the high unpredictability of the core. Conversely, when high-quality raw material is used, knappers adopt more formal technological schemas due to the more predictable raw material.

Specialised studies highlight, for instance, that the Levallois technique is typically associated almost exclusively with flint (Boëda 1994; Tuffreau et al. 2008). Concurrently, the absence of high-quality raw materials within immediate procurement sites is frequently linked to the expedient nature of certain Middle Palaeolithic industries (Geneste 1997; Moncel et al. 2008).

Flint constitutes one of the most suitable raw materials for knapping, regardless of its origin and petrographic typology; therefore, the search for and selection of flint cobbles must have been a common activity among these groups. In an environment such as the one just described for La Sima Cave, this search would entail high energy and time expenditure for what would likely be unsatisfactory results. In fact, in the Middle Palaeolithic sites located along the Guadalquivir River terraces, where the presence of flint lithic industries is common, its provenance has been linked not only to the alluvial deposits themselves but also to the Subbaetic outcrops located more than 30 km away, as observed at the Tarazona II site (Caro et al. 2011).

At the sites located upstream along the Guadaíra River, at the contact zone with the Subbaetic units—as observed at El Rozalejo—the two raw materials used in lithic knapping are local flint and quartzite. Undoubtedly, quartzite cobbles originate from the alluvial deposits of the Guadalquivir River terraces rather than from Palaeozoic quartzite rock outcrops, which are non-existent within the Guadaíra drainage basin (Díaz del Olmo et al. 2023). Its presence is therefore exclusively associated to the anthropogenic introduction of this raw material into geomorphological domains outside the strict Guadalquivir valley; this occurred via the Guadaíra River valley, which forms a geomorphological connecting surface that acted as a regional hominin corridor, at least during the Late Pleistocene, from the end of MIS 6 to MIS 3 (Díaz del Olmo et al. 2023).

Comparing the two situations—Middle Palaeolithic sites located on the mountainous margins of both banks of the Guadalquivir River—reveals a procurement strategy of high-quality quartzites towards both extremities. In the south, this complemented the siliceous rocks collected from the Subbaetic outcrops or within the Guadaíra terraces themselves; in the north (e.g., La Sima Cave), it acted as a higher-quality resource to offset the predominant use of the local lithology, which is represented by quartz. The presence at La Sima Cave of a few flint artefacts highly similar to varieties identified at the Tarazona II site—which have not been detected among the cobbles of the Guadalquivir River terraces—allows us to hypothesise a provenance from the Subbaetic outcrops, a premise that must be verified through expanded sampling and further analytical testing.

Taken together, these data allow the resource catchment area models of the Neanderthal groups at La Sima Cave to be integrated within Middle Palaeolithic mobility patterns. In this context, the use of cost-distance analysis is fundamental for interpreting the behaviour of hunter-gatherer groups, who would have optimised their movements based on the lowest energy expenditure, prioritising cost-effective routes (Surface-Evans and White 2012). The distribution of outcrops within the different isochrones provides insight into the potential mobility strategies of hunter-gatherer groups in this territory. Consequently, the quartz outcrops closest to the site would have been more heavily exploited, whereas those further afield would have required further organised movements due to the greater time and energy investment they entailed.

Geochemical comparison between archaeological artefacts and natural sources constitutes an effective approach for identifying raw material procurement patterns, reconstructing resource exploitation networks, and evaluating the degree of mobility or interaction between human groups and their geological environment. In this regard, although the petrological characterisation of the quartz samples from the different series appears quite homogeneous—as do the knapped lithic pieces—certain variables allow for a more precise assessment of their potential relationship with specific outcrops. Samples CZ1-4 and, most notably, the CZ4 samples are clearly distinct from the rest and have not been detected within the lithic industry. Meanwhile, samples CZ1-1 to CZ1-3 and those from CZ2 exhibit greater similarities to the lithic remains than others, such as CZ3; nonetheless, all of them remain highly similar to the industries found within the cavity.

A range of studies have demonstrated that elemental analysis via X-ray fluorescence techniques, combined with multivariate statistical methods such as principal component analysis or cluster analysis, enables the establishment of associations between archaeological objects and their potential areas of geological origin (Papachristodoulou et al. 2010; Frahm 2013; Wang et al. 2022). The application of these analytical methods at La Sima Cave supports this trend, demonstrating a strong correlation with the samples assigned to the CZ2 and CZ3 series, a weaker association with CZ1, whole definitely excluding the remaining samples.

From a spatial perspective, the accumulated cost map places these quartz outcrops within the blue hues that indicate a low travel effort of less than 120 minutes, as well as within a uniform catchment radius of between 6–7 km. Remarkably, this indicator of low effort extends—albeit with lower intensity—to the vicinity of the Guadalquivir River terraces, suggesting the existence of natural mobility corridors between the site and this fluvial zone. This connection is highly significant given that quartzites from these terraces constitute the second most heavily exploited raw material within La Sima Cave lithic assemblage. A similar pattern could be inferred for flint; however, in this case—and pending a more detailed study—it could even be linked to the circulation of raw materials along the regional hominin corridor defined between the Guadalquivir terraces and the Subbaetic units (Díaz del Olmo et al. 2023).

## Declarations

**Acknowledgements** This article is a contribution to the research projects GeoCroQ (HAR2011-23798), DIVERSO-2 (PID2022-138590NB-C42), CAREQ (funded by the Junta de Andalucía), Research Group PAIDI RNM273: Quaternary and Geomorphology, and the research group INREPA (HUM-262), supported by Línea II (Second Phase of the Applied Research Internal Plan at the University of Córdoba). It also received funding from the CODIRE Project (PP2F_L1_13), financed by the Applied Research Internal Plan of the University of Córdoba with resources from the FEDER-Andalucía Program 2021-2027, as well as from the Sociedad Espeleológica GEOS. We extend our gratitude to the Honorable City Council of Constantina for their support.

**Author contributions** All authors contributed to the conception and design of the study. Material preparation, data collection, and analysis were performed by. Marta Cañete-Gómez, José Antonio Caro-Gómez, César Borja-Barrera, Genaro Álvarez-García, Eusebio J. Medina-Luque, Fernando Díaz Del Olmo, José Manuel Recio-Espejo, María Leticia Gómez-Sánchez and Juan Manuel Garrido-Anguita. The first draft of the manuscript was written by Marta Cañete-Gómez, José Antonio Caro-Gómez and Juan Manuel Garrido-Anguita. All authors commented on previous versions of the manuscript. All authors read and approved the final manuscript.

**Data availability** The unpublished data described correspond to archaeological materials deposited in the Museum of Sevilla. These data are not in open access, as the museum does not have a database of these materials. However, all the materials are available for consultation and analysis in the repository of this institution.

**Conflict of interest** The authors declare no competing interests. During the preparation of this work, the authors used https://www.deepl.com/write and ChatGPT to improve language and readability. Subsequently, they carefully reviewed and refined the content, assuming full responsibility for the final version of the publication.

**Open Access** This article is licensed under a Creative Commons Attribution 4.0 International License, which permits use, sharing, adaptation, distribution and reproduction in any medium or format, as long as you give appropriate credit to the original author(s) and the source, provide a link to the Creative Commons licence, and indicate if changes were made. The images or other third-party material in this article are included in the article's Creative Commons licence, unless indicated otherwise in a credit line to the material. If material is not included in the article's Creative Commons licence and your intended use is not permitted by statutory regulation or exceeds the permitted use, you will need to obtain permission directly from the copyright holder. To view a copy of this licence, visit http://creativecommons.org/licenses/by/4.0/.

## References

1. Abrunhosa A (2020) Proveniência das matérias-primas e a sua relação com a tipologia: estudo do conjunto lítico Moustiesenre dos sítios arqueológicos do Calvero de la Higuera (Madrid, Espanha). Ph.D. dissertation, Universidade do

Algarve, Faro, Portugal.

2. Abrunhosa A, Pereira T, Márquez B, Baquedano E, Arsuaga JL, Pérez-González A (2019) Understanding Neanderthal technological adaptation at Navalmaíllo Rock Shelter (Spain) by measuring lithic raw materials performance variability. Archaeol Anthropol Sci 11:5949–5962. https://doi.org/10.1007/s12520-019-00826-3
3. Álvarez G, Rodríguez J, Rodrigo JM, Molina J, Caro JA, Vera AL, Buendía AF, Cáceres L, Martínez A, Algora C, Alcaraz JM, López JA, Riquelme JA, Recio JM, Núñez MA (2005) Noticia sobre dos proyectos de investigación espeleológica: Cueva de los Covachos (Almadén de la Plata) y Cueva La Sima (Constantina). Actas del IX Congreso Español de Espeleología, pp. 151–167.
4. Ambrose S, Lorenz K (1990) Social and ecological models for the middle stone age in southern Africa. In: The emergence of modern humans: An archaeological perspective. Edinburgh University Press, Edinburgh, pp. 3–33. https://doi.org/10.1515/9781474470957-003
5. Andrefsky W Jr (1994) The geological occurrence of lithic material and stone tool production strategies. Geoarchaeology 9:375–391. https://doi.org/10.1002/gea.3340090503
6. Arteaga-Brieba A, Mosquera M, Ollé A (2026) A matter of choice: Raw material specialisation at the Middle Pleistocene kill-butchering site of Gran Dolina TD10.2 Atapuerca, Spain. Quat Int 765:110221. https://doi.org/10.1016/j.quaint.2026.110221
7. Aubry T, Gameiro C, Mangado Llach J, Luis J, Matias H, Do Pereiro T (2016) Upper Palaeolithic lithic raw material sourcing in Central and Northern Portugal as an aid to reconstructing hunter-gatherer societies. J Lithic Stud 3(2):7–28. https://doi.org/10.2218/jls.v3i2.1436
8. Aubry T, Barbosa AF, Gameiro C, Luis L, Santos AT, Silvestre M (2022) Far from flint: Inferring land-use and social networks from Middle and Upper Palaeolithic lithic assemblages (Cardina-Salto do Boi, Côa Valley, Portugal). J Archaeol Sci Rep 42:103385. https://doi.org/10.1016/j.jasrep.2022.103385
9. Baena J, Bárez S, Pérez-González A, Roca M, Lázaro A, Márquez R, Rus I, Manzano C, Cuartero F, Ortiz I, Rodríguez P, Pérez T, González I, Polo J, Rubio D, Alcaraz M, Escobar A (2011) Searchers and miners: First signs of flint exploitation in Madrid's region. In: Capote M, Consuegra S, Díaz-del-Río P, Terradas X (eds) Proceedings of the 2nd International Conference of the UISPP Commission on Flint Mining in Pre- and Protohistoric Times (Madrid, 14–17 October 2009). Archaeopress Publishers of British Archaeological Reports, Oxford.
10. Belmiro J, Terradas X, Dominguez-Bella S, Cascalheria J (2025) Within and Beyond: Chert Procurement Patterns During The Upper Palaeolithic in Southwesternmost Iberia. J Paleo Arch 8:8. https://doi.org/10.1007/s41982-025-00209-2
11. Boëda E (1994) Le Concept Levallois: Variabilité Des Méthodes. Monographie Du CRA, vol 9. CNRS Éditions, Paris.
12. Brantingham PJ (2006) Measuring forager mobility. Curr Anthropol 47(3):435–459. https://doi.org/10.1086/503062
13. Browne CL, Wilson L (2011) Resource selection of lithic raw materials in the Middle Palaeolithic in southern France. J Hum Evol 61(5):597–608. https://doi.org/10.1016/j.jhevol.2011.08.004
14. Burke A (2012) Spatial abilities, cognition and the pattern of Neanderthal and modern human dispersals. Quat Int 247:230–235. https://doi.org/10.1016/j.quaint.2010.10.029
15. Caro JA, Díaz del Olmo F, Cámara R, Recio JM, Borja C (2011) Geoarchaeological alluvial terrace system in Tarazona: Chronostratigraphical transition of Mode 2 to Mode 3 during the middle-upper pleistocene in the Guadalquivir River valley (Seville, Spain). Quat Int 243:143–160. https://doi.org/10.1016/j.quaint.2011.04.022
16. Caro JA, Álvarez G, Molina J, Rodrígo JM, Buendía AF (2013) Recuperación de la memoria arqueológica del yacimiento prehistórico cueva La Sima (Constantina, Sevilla). ANTIQVITAS 25:49–60.
17. Caro JA, Álvarez G, Borja C, Recio JM, Martínez A, Riquelme JA (2017) Prehistoria y patrimonio en la oscuridad: registro arqueológico en cuevas de la Sierra Norte de Sevilla. In: XI Jornadas de Patrimonio Histórico y Cultural de la Provincia de Sevilla. El patrimonio subterráneo (natural o artificial) en la provincia de Sevilla. Diputación de Sevilla, Sevilla, pp. 55–71.
18. Caro JA, Medina EJ, Borja C, Díaz del Olmo F, Recio JM (2023) Paleolítico Antiguo en las terrazas medias del río Guadalquivir: Contexto geomorfológico y análisis tecnológico de la industria lítica del yacimiento de Algabarrilla (Carmona, Sevilla, SO de España). In: Garrido Anguita JM (ed) Conexiones Culturales y Patrimonio Prehistórico. Archaeopress, Oxford, pp. 212–234. https://doi.org/10.2307/j.ctv37c06c2.20

19. Caro-Gómez JA, Borja-Barrera C, Medina-Luque EJ, Cañete-Gómez M, Álvarez-García G, Díaz del Olmo F, Recio-Espejo JM, Riquelme-Cantal JA, Ruiz-Expósito A, Garrido-Anguita JM (2026) Geoarchaeology at La Sima Cave. A multi-analysis approach to the Middle Paleolithic during MIS 3 in southern Iberia. Quat Int 764:110209. https://doi.org/10.1016/j.quaint.2026.110209
20. Carriazo JM (1974) Protohistoria de Sevilla. Guadalquivir S.L. Ediciones, Sevilla.
21. Costa M, Dias L, Rocha L, Oliveira J, Barrulas P, Mirão J (2022) Lithic arrowheads: Siliceous raw material sources and technology in Southern Portugal. Geoarchaeology 37(3):560–573. https://doi.org/10.1002/gea.21891
22. De Lombera-Hermida A, Rodríguez XP, Fábregas R, Moncel MH (2011) La gestion du quartz au Pléistocéne moyen et supérieur. Trois exemples d'Europe Méridionale. L'Anthropologie 115:294–331. https://doi.org/10.1016/j.anthro.2011.02.003
23. De Lombera-Hermida A, Rodríguez-Álvarez XP, Iglesias AA, Díaz M, Valverde I, Pérez-Alberti A, Cunha PP, Ba García H, Aldea X, Lorenzo C, Mosquera T, Fábregas R (2021) Between two worlds: Cova eirós and the middle-upper Palaeolithic transition in NW Iberia. CR Palevol 20:859–886. https://doi.org/10.5852/cr-palevol2021v20a4
24. Díaz del Olmo F, Caro JA, Borja C, Recio JM, Cámara R, Martínez A (2023) Hominid Alluvial Corridor (HAC) of the Guadalquivir and Guadaíra River Valleys (Southern Spain): Geoarchaeological Functionality of the Middle Paleolithic Assemblages during the Upper Pleistocene. Geosciences 13:206. https://doi.org/10.3390/geosciences13070206
25. Dibble HL (1991) Local raw material exploitation and its effects on Lower and Middle Paleolithic assemblage variability. In: Montet-White A, Holen S (eds) Raw material economies among prehistoric hunter-gatherers. University of Kansas, Publications in Anthropology, vol 19, pp 33–48.
26. Eixea A, Roldán C, Villaverde V, Zilhão J (2014) Middle Palaeolithic flint procurement in Central Mediterranean Iberia: Implications for human mobility. J Lithic Stud 1(1):103–115. https://doi.org/10.2218/jls.v1i1.783
27. Féblot-Augustins J (1993) Mobility strategies in the Late Middle Palaeolithic of central Europe and western Europe: elements of stability and variability. J Anthropol Archaeol 12:211–265. https://doi.org/10.1006/jaar.1993.1007
28. Féblot-Augustins J (1999) Raw material transport patterns and settlement systems in the European Lower and Middle Palaeolithic: continuity, change and variability. In: Roebroeks W, Gamble C (eds) The Middle Palaeolithic Occupation of Europe. University of Leiden, Leiden, pp. 193–214.
29. Fernandes P, Raynal JP (2007) Pétroarchéologie du silex. In: Raynal JP (ed) Sainte-Anne I, Sinzelles, Polignac, Haute-Loire. Le Paléolithique moyen de l´unité J1, Les Dossiers de l'Archéo-Logis, vol 3. Archéo-Logis/CDERAD, Laussonne, pp. 59–98.
30. Fernandes P, Raynal JP, Moncel MH (2008) Middle Palaeolithic raw material gathering territories and human mobility in the southern Massif Central, France: first results from a petro-archaeological study on flint. J Archaeol Sci 35(8):2357–2370. https://doi.org/10.1016/j.jas.2008.02.012
31. Forster N, Grave P, Vickery N, Kealhofer L (2011) Non-destructive analysis using PXRF: methodology and application to archaeological ceramics. X-Ray Spectrom 40:389–398. https://doi.org/10.1002/xrs.1360
32. Frahm E (2013) Validity of "off-the-shelf" handheld portable XRF for sourcing Near Eastern obsidian chip debris. J Archaeol Sci 40(2):1080–1092. https://doi.org/10.1016/j.jas.2012.06.038
33. Gamble C (1999) The Palaeolithic Societies of Europe. Cambridge University Press, Cambridge.
34. Garcia-Rojas M, Dominguez-Ballesteros E, Prieto A, Calvo A, Sánchez A, Tarrino A, Arrizabalaga A (2021) A great step forward. Lithic raw material procurement and management among Palaeolithic hunter-gatherers in the Basque crossroads. J Lithic Stud 7(2). https://doi.org/10.2218/jls.5434
35. Geneste JM (1985) Analyse lithique d'industries moustériennes du Périgord: Une approche technologique du comportement des groupes humains au Paléolithique moyen. PhD Dissertation, University of Bordeaux I.
36. Geneste JM (1988) Les industries de la grotte Vaufrey: technologie du débitage, économie et circulation de la matière première. In: Rigaud JP (ed) La grotte Vaufrey. Paléoenvironnement, chronologie, actividades humaines. Mémoire de la Société Préhistorique Française, XIX, pp. 441–519.
37. Geneste JM (1992) Systèmes techniques de production lithique: variations technoéconomiques dans les processus de réalisation des outillages paléolithiques. Techniques et culture 17-18:1–35. https://doi.org/10.4000/tc.683
38. Geneste JM, Jaubert J, Lenoir M, Meignen L, Turq A (1997) Approche technologique des Moustériens charentiens du sud-ouest de la France et du Languedoc oriental. Paleo 9:101–142. https://doi.org/10.3406/pal.1997.1230

39. Gomez de Soler BG, Soto M, Vallverdu J, Bargallo A, Chacon MG, Romagnoli F, Vaquero M (2020) The Panadella chert (Montmaneu Formation): A high-quality raw material in the Abric Romani sequence (NE Iberian Peninsula). Archaeol Anthropol Sci 12(11):252. https://doi.org/10.1007/s12520-020-01198-9
40. Goodman ME (1944) The physical properties of stone tool materials. Am Antiq 9(4):415–433. https://doi.org/10.2307/275093
41. Karlin C, Bodu P, Pelegrin J (1991) Processus techniques et chaînes opératoires. Comment les préhistoriens s'approprient un concept élaboré par les ethnologues. In: Balfet H (ed) Observer l'action technique: des chaînes opératoires, pour quoi faire? Éditions du CNRS, Paris, pp. 101–117.
42. Kelly RL (1983) Hunter-gatherer mobility strategies. J Anthropol Res 39:277–306. https://doi.org/10.1086/jar.39.3.3629672
43. Kuhn SL (1991) "Unpacking" reduction: Lithic raw material economy in the mousterian of west-central Italy. J Anthropol Archaeol 10(1):76–106. https://doi.org/10.1016/0278-4165(91)90022-P
44. Kuhn SL (1995) Mousterian Lithic Technology: An Ecological Perspective. Princeton University Press, Princeton.
45. Kuhn SL (2004) Upper Paleolithic raw material economies at Ucağızlı cave, Turkey. J Anthropo Archaeol 23(4):431–448. https://doi.org/10.1016/j.jaa.2004.09.001
46. Kuhn SL (2020) Moving on from Here: Suggestions for the Future of "Mobility Thinking" in Studies of Paleolithic Technologies. J Paleolith Archaeol 3(4):664–681. https://doi.org/10.1007/s41982-020-00060-7
47. Lemonnier P (1976) La description des chaînes opératoires: contribution à l'analyse des systèmes techniques. Techniques & Culture 1:100–151. https://doi.org/10.4000/tc.6267
48. Lemonnier P (1986) The study of material culture today: toward an anthropology of technical systems. J Anthropol Archaeol 5(2):147–186. https://doi.org/10.1016/0278-4165(86)90012-7
49. Leroi-Gourhan A (1964) Le geste et la parole: Technique et langage. Albin Michel, Paris.
50. Melo MNR, Deschamps M, Zilhão J (2025) The Middle Paleolithic quartz assemblage from Gruta da Figueira Brava (Portugal). CR Palevol 24(28):563–585. https://doi.org/10.5852/cr-palevol2025v24a28
51. Moncel MH, Brugal JP, Prucca A, Lhomme G (2008) Mixed occupation during the Middle Palaeolithic: case study of a small pit-cave-site of Les Pêcheurs (Ardèche, south-eastern France). J Anthropol Archaeol 27(3):382–398. https://doi.org/10.1016/j.jaa.2008.03.005
52. Moncel MH, Fernandes P, Chacón MG, De Lombera A, Menendez L, Youcef S, Moigne AM, Patou-Mathis M, Daujeard C, Rivals F, Theodoropoulou A, Valladas H, Mercier N, Bahain JJ, Voinchet P, Falguères C, Michel V, Guanjun C, Yokoyama Y, Combier J (2014) Emergence et diversification des stratégies au Paléolithique moyen ancien (350 000 à 120 000 ans) dans la vallée du Rhône (France). Les sites d'Orgnac 3 et Payre. In: Brenet M, Bourguignon L, Jarry M (eds) Emergence et Diversité Des Techno-Complexes Du Paléolithique Moyen Ancien. Société Préhistorique Française, Bordeaux, pp. 59–81.
53. Moncel MH, Chacón MG, Vettese D, Courty MA, Daujeard C, Eixea A, Fernandes P, Allué E, Hardy B, Rivals F, Béarez P, Gallotti R, Puaud S (2021) Late Neanderthal short-term and specialized occupations at the Abri du Maras (South-East France, level 4.1, MIS 3). Archaeol Anthropol Sci 13, 45. https://doi.org/10.1007/s12520-021-01285-5
54. Mourre V (1996) Les industries en quartz au Paléolithique. Terminologie, méthodologie et technologie. Paleo 8:205–223. https://doi.org/10.3406/pal.1996.1160
55. Navazo Ruiz M, Jordá Pardo JF, Burow C, Kehl M, Pastoors A, Weniger GC, Wood R (2020) Last Neanderthal Occupations at Central Iberia: the Lithic Industry of Jarama VI Rock Shelter (Valdesotos, Guadalajara, Spain). Archaeol Anthropol Sci 12, 45. https://doi.org/10.1007/s12520-019-00974-6
56. Papachristodoulou C, Gravani K, Oikonomou A, Ioannides K (2010) On the provenance and manufacture of red-slipped fine ware from ancient Cassope (NW Greece): Evidence by X-ray analytical methods. J Archaeol Sci 37:2146–2154. https://doi.org/10.1016/j.jas.2010.02.013
57. Peña L (2008) Morpho-technological study of the Lower and Middle Palaeolithic lithic assemblages from Maltravieso and Santa Cave (Cáceres, Extremadura). Comparison of two lithic assemblages knapped in milky quartz: Maltravieso cave- Sala de los Huesos- and level C of L'Arago cave (Tautavel, France). Annali dell'Università degli Studi di Ferrara: Museologia Scientifica e Naturalistica, Vol speciale. https://doi.org/10.15160/1824-2707/496
58. Picin A, Chacón MG, Gómez de Soler B, Blasco R, Rivals F, Rosell J (2020) Neanderthal mobile toolkit in short-term occupations at Teixoneres Cave (Moia, Spain). J Archaeol Sci Rep 29:102165. https://doi.org/10.1016/j.jasrep.2019.102165

59. Uzunidis A, Blasco R, Brugal JP, Fourcade T, Ochando J, Rosell J, Roussel A, Rufà A, Sánchez MF, Texier PJ, Rivals F, (2024) Neanderthal hunting grounds: The case of Teixoneres Cave (Spain) and Pié Lombard rockshelter (France). J Archaeol Sci 168:106007. https://doi.org/10.1016/j.jas.2024.106007
60. Potts PJ, Webb PC, Watson JS (1985) Energy-dispersive X-ray fluorescence analysis of silicate rocks: comparisons with wavelength-dispersive performance. Analyst 110 (5):507–513.https://doi.org/10.1039/AN9851000507
61. Prieto A, Yusta I, Pastoors A, Claßen E (2019) Petrological characterisation of the "Tertiary quartzites" from the site of Troisdorf-Ravensberg (North Rhine-Westphalia, Germany): First insights in Middle Palaeolithic outcrop exploitation. Quartär 66:33–50. https://doi.org/10.7485/QU66_2
62. Renfrew C (1984) Approaches to social archaeology. Edinburgh University Press, Edinburgh.
63. Riquelme-Cantal JA, Caro-Gómez JA, Garrido-Anguita JM, Borja C, Álvarez G, Díaz del Olmo F, Recio JM, Ruiz A, Martín de la Cruz JC, Ávila R, Rivas MM (2025) Caves as Refuge for Hominids and Carnivores in the Mousterian of the Southern Iberia Peninsula. In: Cortés-Sánchez M, Simón-Vallejo MD, Pablos Fernández A (eds) Neandertals at the End of the World. New Perspectives for Iberia, SPAL Monografías Arqueología, vol LVII. Universidad de Sevilla, Sevilla, pp. 79–89. https://hdl.handle.net/11441/177916
64. Rodríguez J, Cáceres LM, Álvarez G, Martínez A, Alcaraz JM, Riquelme JA, Recio JM (2003) Secuencia cronoestratigráfica del Pleistoceno Superior en Sierra Morena: la Cueva de La Sima (Constantina, Sevilla). Geogaceta 33:47–50.
65. Roebroeks W (1988) From find scatters to early hominid behaviour: a study of Middle Palaeolithic riverside settlements at Maastricht-Belveder (The Netherlands). Analecta Praehistorica Leidensia 21.
66. Rolland N, Dibble HL (1990) A new synthesis of Middle Paleolithic assemblage variability. Am Antiq 55(3):480–499. https://doi.org/10.2307/281279
67. Sanchez de la Torre M, Mangado X, Castillo-Jimenez S, Luque L, Alcolea-González JJ, Alcaraz-Castaño M (2023) New data on chert catchment analysis in inland Iberia during the Late Pleistocene. Geoarchaeology. https://doi.org/10.1002/gea.21963
68. Shackley MS (2020) X-Ray Fluorescence (XRF): Applications in Archaeology. In: Smith C (ed) Encyclopedia of Global Archaeology. Springer, Cham. https://doi.org/10.1007/978-3-030-30018-0_1305
69. Slimak L, Giraud Y (2007) Circulations sur plusieurs centaines de kilomètres durant le Paléolithique moyen. Contribution à la connaissance des sociétés néandertaliennes. CR Palevol 6(5):359–368. https://doi.org/10.1016/j.crpv.2007.06.001
70. Soressi M, Geneste JM (2011) Special Issue: Reduction Sequence, Chaîne Opératoire, and Other Methods; the Epistemologies of Different Approaches to Lithic Analysis; the History and Efficacy of the Chaîne Opératoire Approach to Lithic Analysis; studying Techniques to Reveal Past Societies in an Evolutionary Perspective. PaleoAnthropology 2011:334–350. https://doi.org/10.4207/PA.2011.ART63
71. Strauss LG (1991) The role of raw materials in upper Paleolithic and Mesolithic stone artifact assemblage variability in Southwest Europe. In: Montet-White A, Holen S (eds) Raw material economies among prehistoric Hunter-Gatherers. University of Kansas, Publications in Anthropology, pp. 185–190.
72. Surface-Evans SL, White DA (2012) An Introduction to the Least Cost Analysis of Social Landscapes. In: Surface-Evans SL, White DA (eds) Least Cost Analyses of Social Landscapes: Archaeological case studies, University of Utah Press, pp. 1–10.
73. Tobler WR (1993) Non-isotropic geographic modeling. NCGIA Technical Report 93-4, National Center for Geographic Information and Analysis.
74. Tuffreau A, Lamotte A, Goval E (2008) Les industries acheuléennes de la France Septentrionale. L'Anthropologie 112:104–139. https://doi.org/10.1016/j.anthro.2008.01.003
75. Verhagen P, Brughmans T, Nuninger L, Bertoncello F (2014) The long and winding road: Combining Least Cost Paths and Network Analysis Techniques for Settlement Location Analysis and Predictive Modelling. In: CAA2012 Proceedings of the 40th Conference in Computer Applications and Quantitative Methods in Archaeology, Southampton, pp. 357–366. https://doi.org/10.1017/9789048519590.039
76. Villeneuve Q, Faivre JP, Turq A, Guadelli JL (2019) Étude techno-économique du Moustérien de Pradayrol (Caniac-du-Causse, Lot): entre mobilité des ressources lithiques et adaptation aux materiales locaux, un exemple de gestion complémentaire des quartz et silex au Paléolithique moyen récent en Quercy. CR Palevol 18(2):251–267. https://doi.org/10.1016/j.crpv.2018.10.002

77. Vita-Finzi C, Higgs ES, Sturdy D, Harriss J, Legge AJ, Tippett H (1970) Prehistoric economy in the Mount Carmel area of Palestine: site catchment analysis. Proc Prehist Soc 36:1–37. https://doi.org/10.1017/S0079497X00013074
78. Wang Z, Zhang Z, Wang F, Liu J (2022) A pXRF-Based Approach to Identifying the Material Source of Stone Cultural Relics: A Case Study. Minerals 12(2):199. https://doi.org/10.3390/min12020199
79. Wheatley D, Gillings M (2002) Spatial Technology and Archaeology: The Archaeological Applications of GIS. Taylor & Francis. https://doi.org/10.1201/b12806
80. Wilson L (2007) Terrain difficulty as a factor in raw material procurement in the Middle Palaeolithic of France. J Field Archaeol 32:315–324. https://doi.org/10.1179/009346907791071539

## Figures

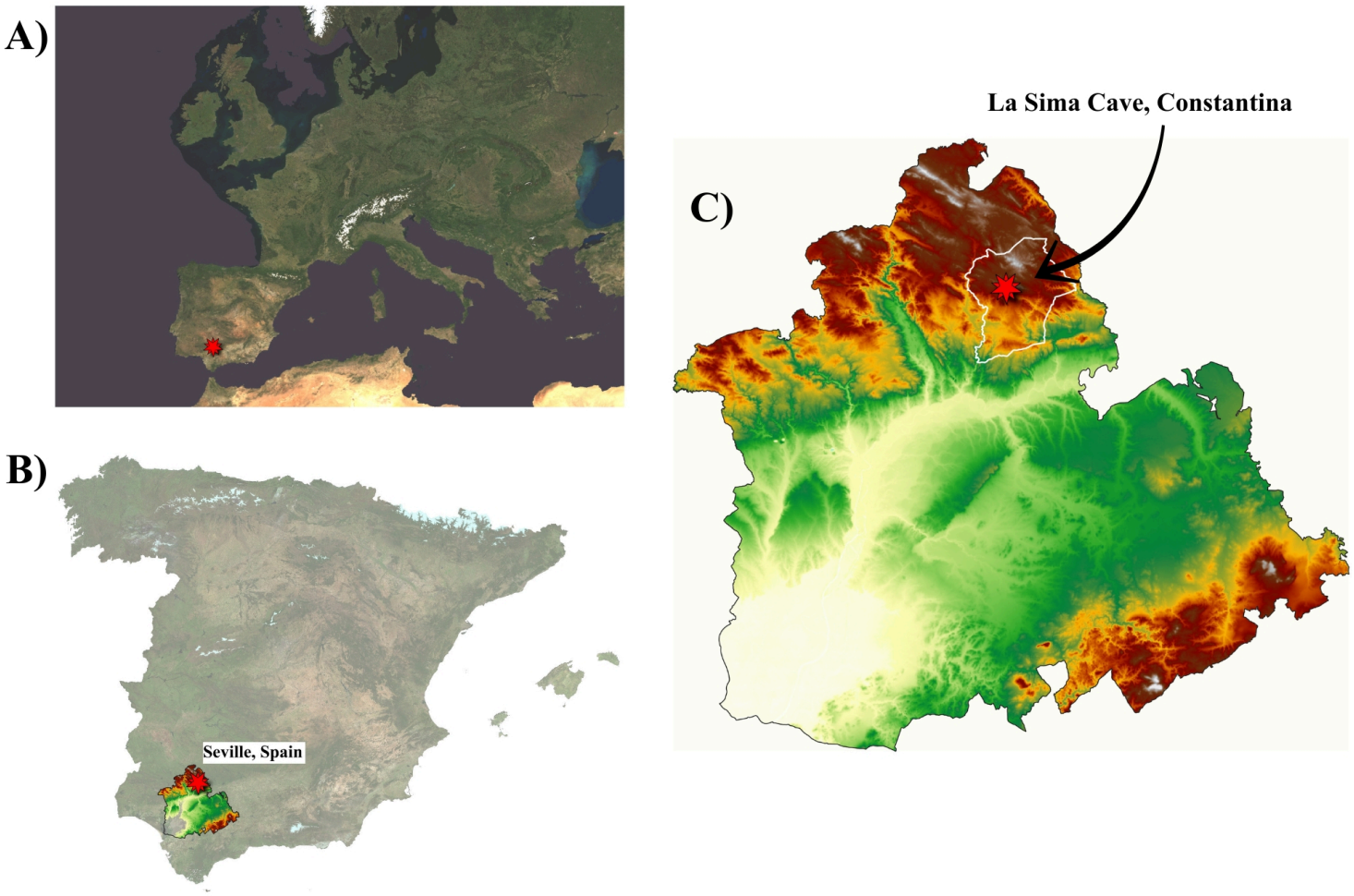



**Figure 1**

General location of the study area within its continental (A), peninsular (B), and provincial (C) contexts.

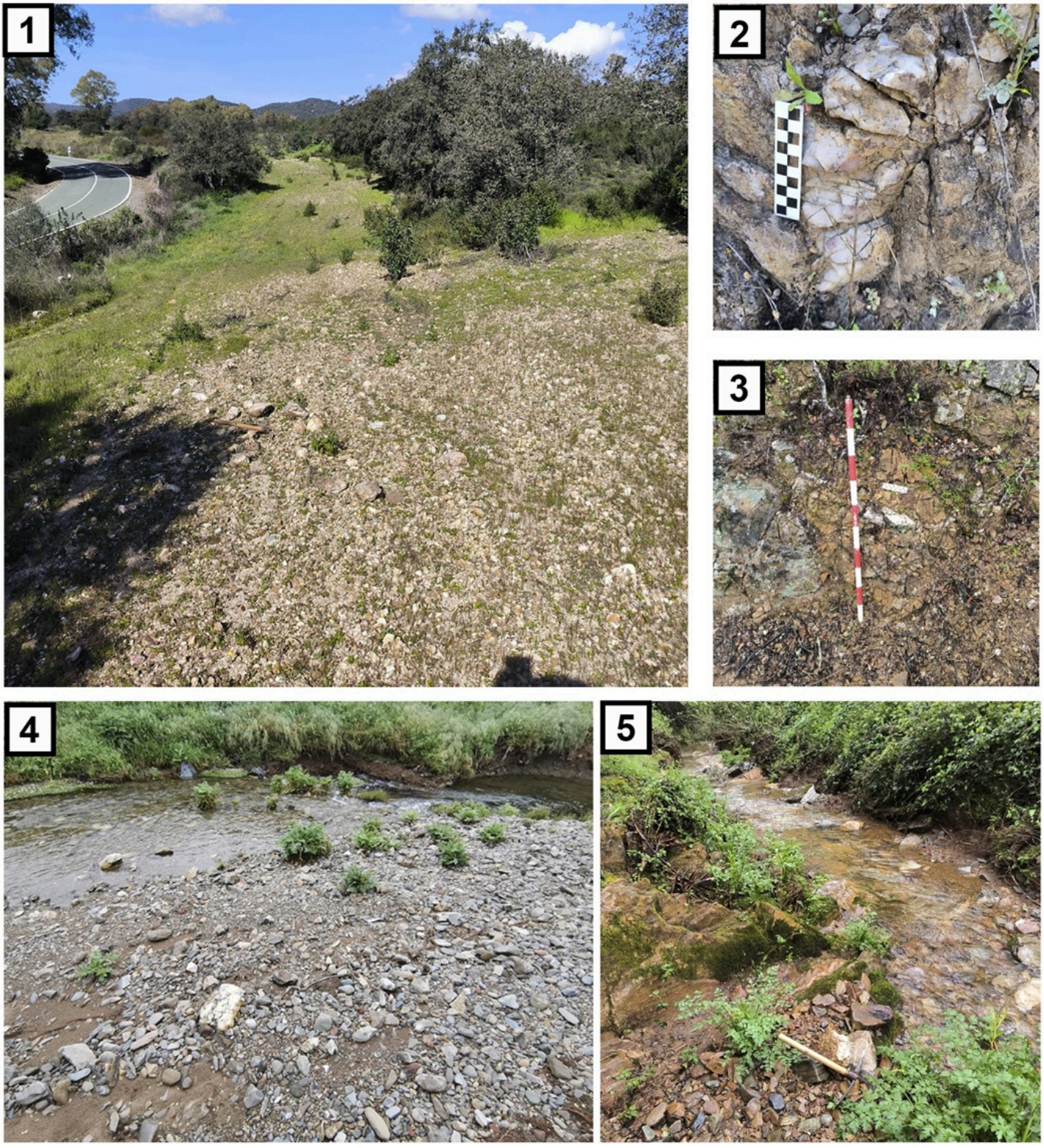



**Figure 2**

Quartz procurement sites in the vicinity of La Sima Cave. Quartz vein outcrops: 1) Tierras Nuevas, CZ1; 2) Castillo de Setefilla, CZ5; 3) Sierra de los Ganazos, CZ4. Accumulation of blocks and cobbles in local streams and rivers. 4) Malpicas, CZ3; 5) Las Majadillas, CZ2.

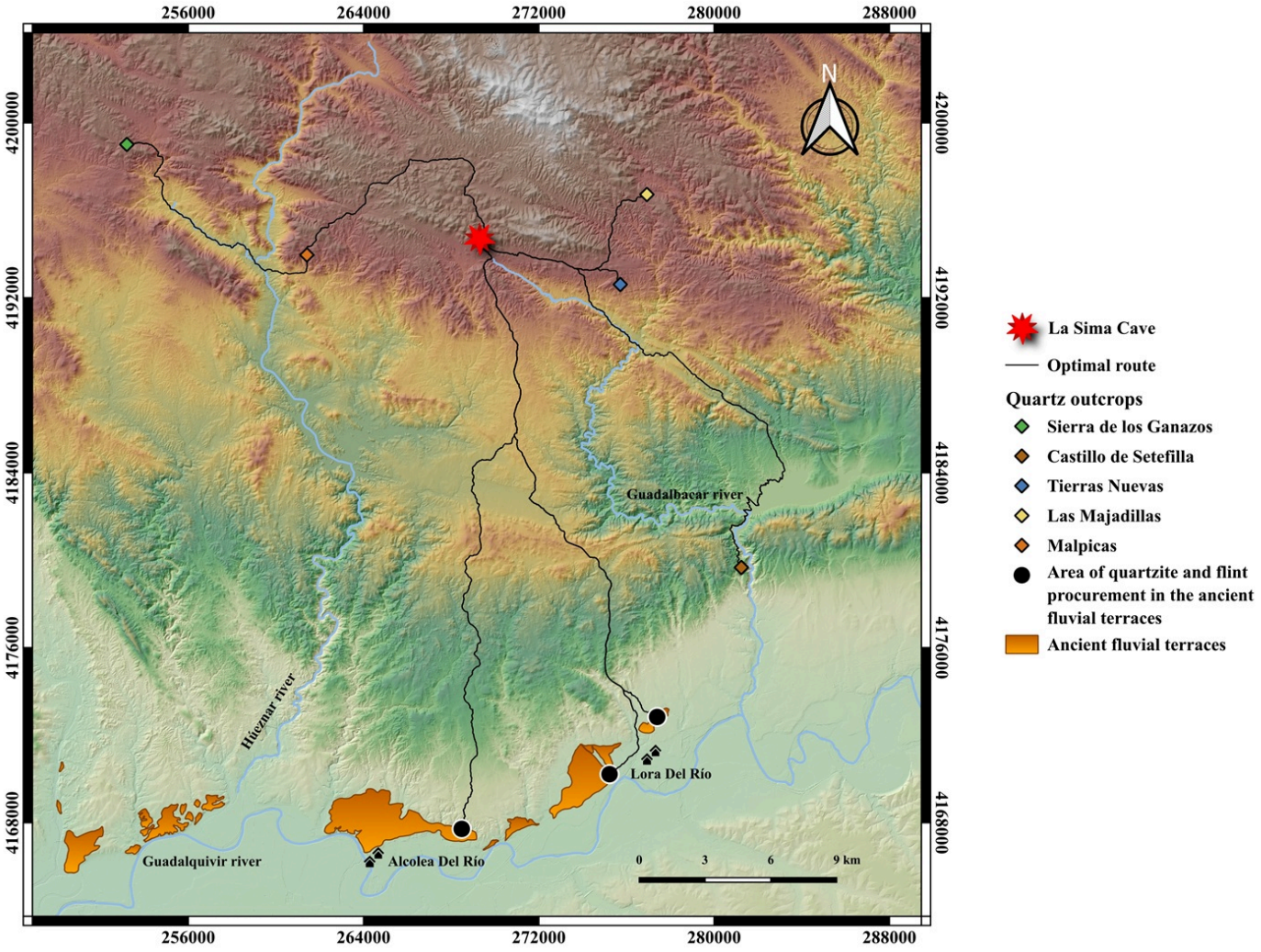



**Figure 3**

Least-cost paths map identifying the optimal routes and geographical difficulty between La Sima Cave and the various raw material outcrops.

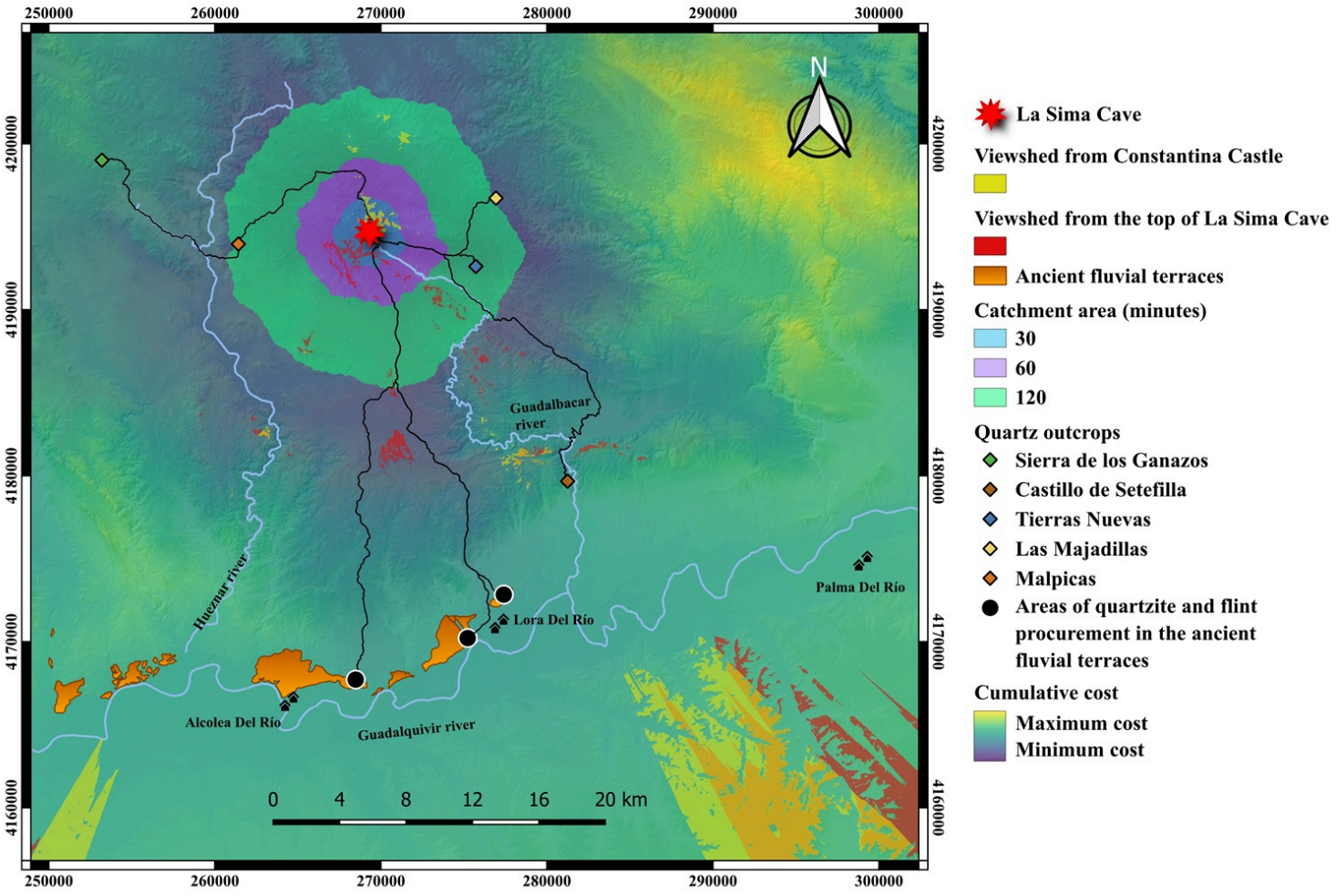



**Figure 4**

Map displaying the viewshed from La Sima Cave, the accumulated cost (energy expenditure required to travel from the site to any point in the territory), and the travel time intervals.

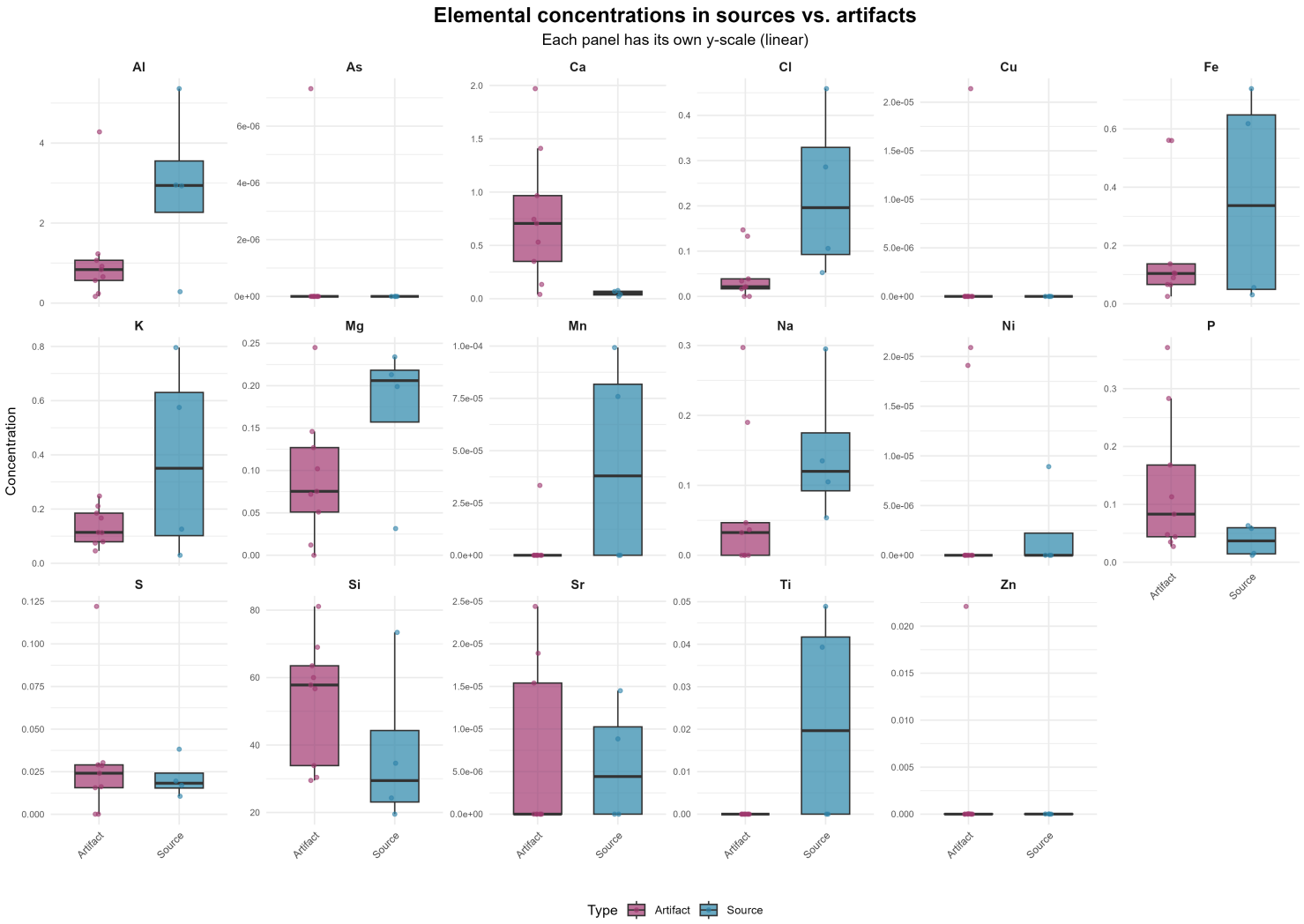



**Figure 5**

Faceted boxplots displaying the distribution of elemental concentrations (in wt.%) for the source area samples (CZ, in blue) and archaeological artefacts (SIM, in red).

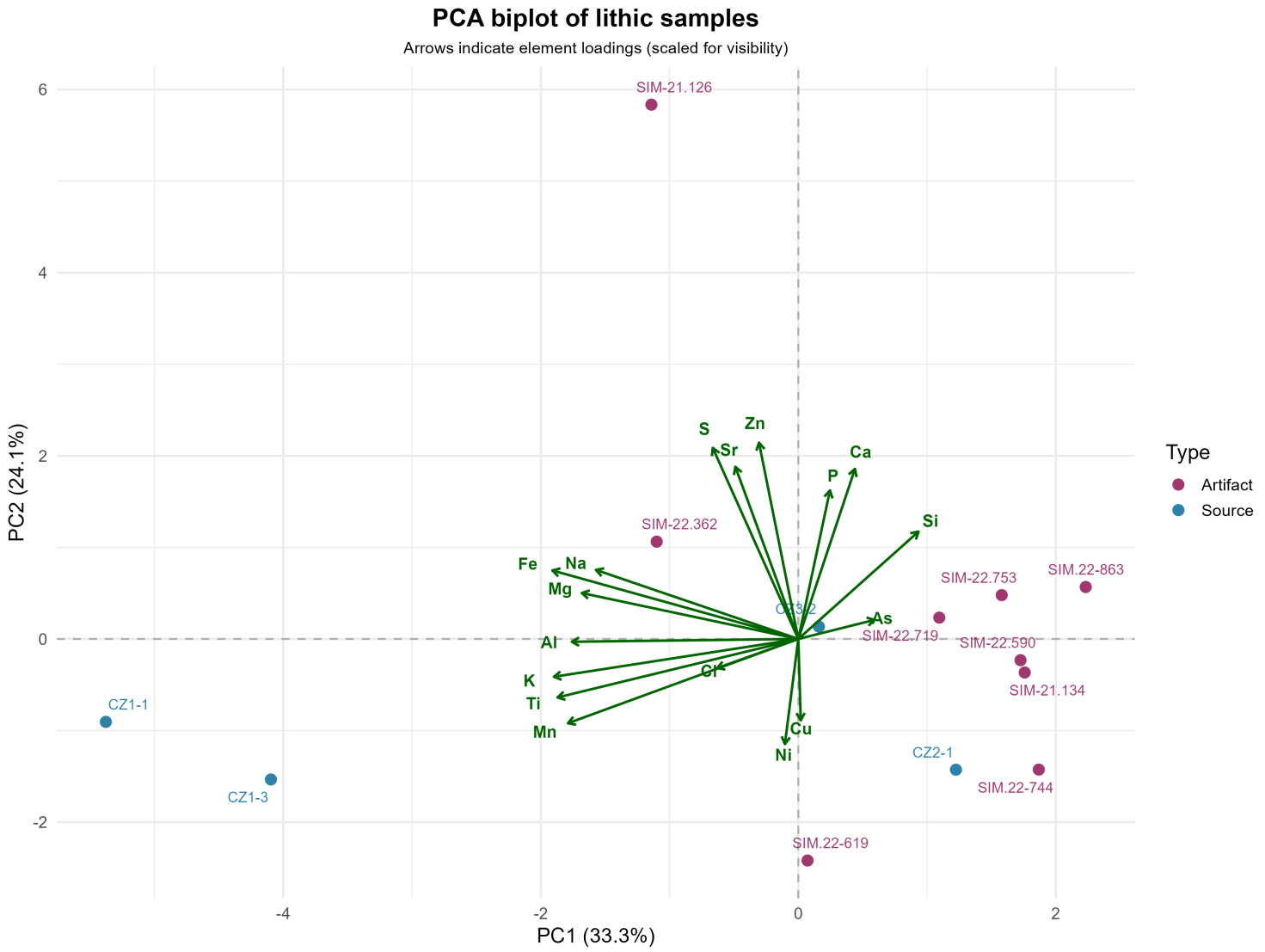



**Figure 6**

Principal Component Analysis (PCA) biplot of the standardised elemental data, displaying sample (scores) and variable (loadings).

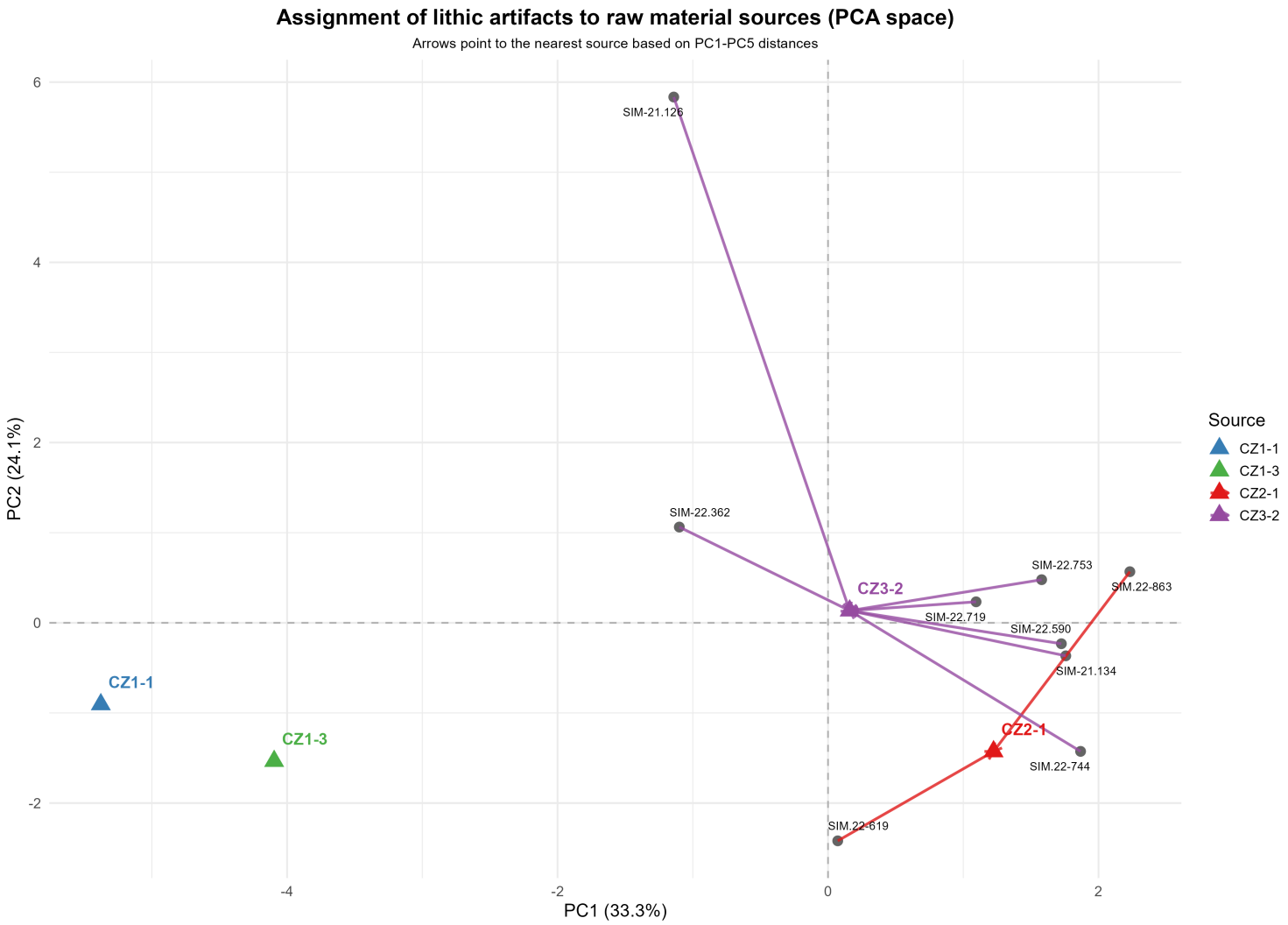



**Figure 7**

Map of archaeological artefact assignment to raw material sources on the PCA PC1–PC2 plane. The arrows connect each artefact (grey circles) to the nearest source in the space of the first five principal components (minimum Euclidean distance)

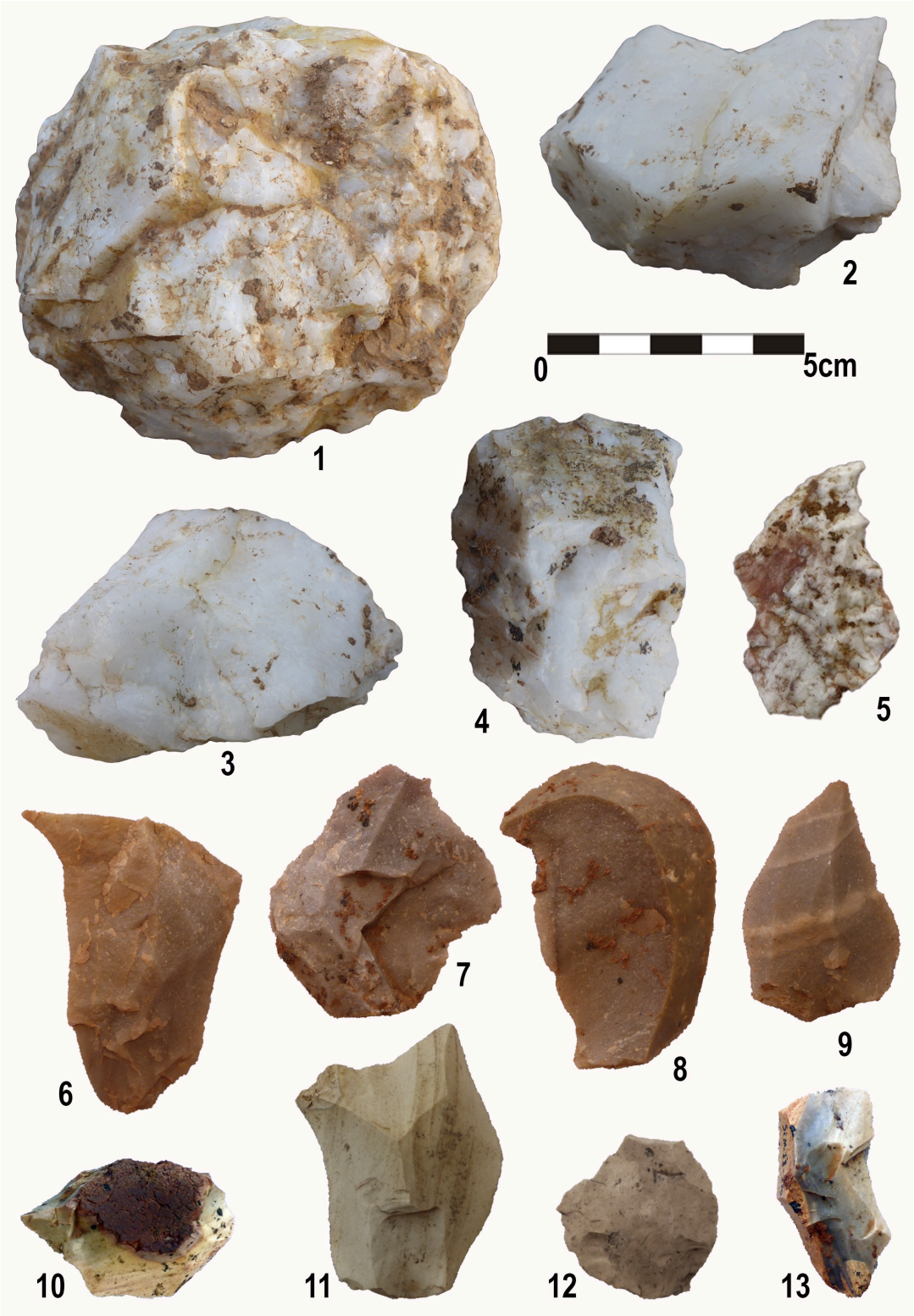



**Figure 8**

Lithic industry from La Sima Cave (Constantina, Seville). Quartz: Cores (1 to 4), denticulates (5), Quartzite: Flakes (6 to 8), Levallois points (9), Flint: Flakes (10, 11 and 13), and Levallois flake (12). GAU 4 (5, 6, 7 and 11); and GAU 5 (1, 2, 3, 4, 8, 9 and 10).

## Supplementary Files

This is a list of supplementary files associated with this preprint. Click to download.

- Supplementarymaterial.rar